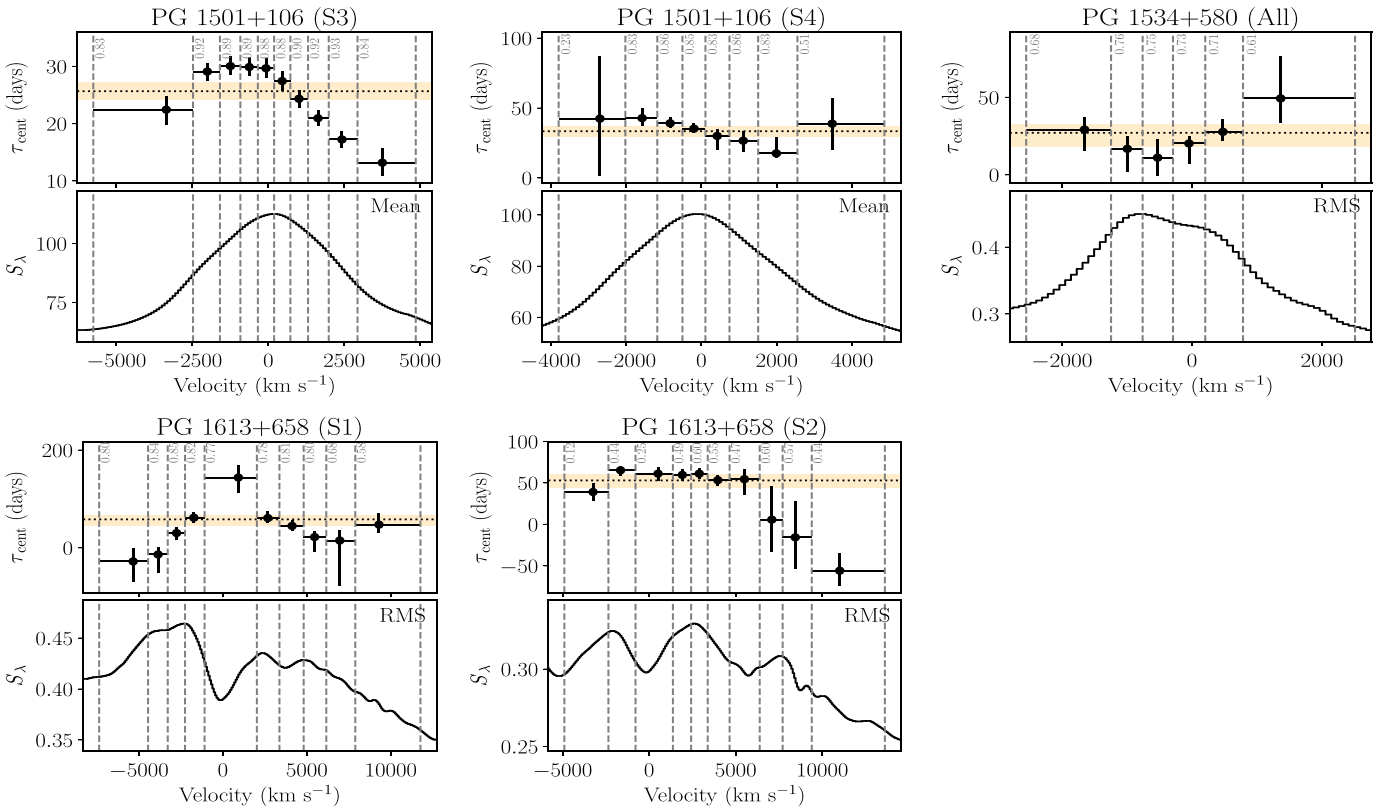

Figure 18. (Continued.)

PG 1048+342: The profile of its broad Hβ shows a more significant red asymmetry compared to the profiles in Boroson & Green (1992) and Kaspi et al. (2000), but it displayed no significant changes over the four seasons in our campaign. Kaspi et al. (2000) did not manage to sample this object sufficiently to successfully measure the time lag of its Hβ line. The clear variation (especially in Season 1 and in the entire light curve) enables us to give a reliable measurement of its Hβ time lag for the first time. The time lag measured from the entire light curve ($36.8^{+2.4}_{-3.4}$ days) using MICA has smaller uncertainties than that from Season 1 ($28.0^{+5.6}_{-4.8}$ days) and is thus preferred for the BH mass determination, which we calculate to be $4.44^{+0.31}_{-0.42} \times 10^7 M_\odot$. The longer lags at blue velocities and shorter lags at red velocities measured from Season 1 show the signature of inflow.

PG 1100+772 (3C 249.1): Although the variability of Hβ ($F_{\rm var} = 1.6\%$) is much smaller than that of the 5100 Å continuum flux ($F_{\rm var} = 8.9\%$, see Table 3), we can still measure a Hβ time lag using MICA. The ICCF and χ^2 methods cannot give reliable measurements to the lags because of the small line variation amplitude. The profile of its broad Hβ shows clear red asymmetry. The time lag measured from the entire light curve is $55.9^{+3.0}_{-1.4}$ days and the BH mass is $7.81^{+0.54}_{-0.47} \times 10^8 M_\odot$. It is a radio-loud object (Fanaroff–Riley II) with asymmetric radio lobes and has an extended emission-line region. Its jets and its extended emission-line region were suggested to originate from the merger of the host galaxy of a gas-poor quasar and a large late-type galaxy (Stockton & Mackenty 1983; Gilbert et al. 2004; Fu & Stockton 2009). Because of the small variation of Hβ flux, the profile of the rms spectrum is poorly constrained. The lags at different velocities are only marginally resolved. On average, the lags at blue velocities are shorter than those in the red, which may indicate an outflow (not on a significant scale because of the small variation amplitude).

PG 1202+281 (GQ Com): The Hβ time lag is reported here for the first time. The profile of its broad Hβ shows a red asymmetry. The peak of Hβ was blueshifted in previous spectra from Boroson et al. (1985), Boroson & Green (1992), Kaspi et al. (2000), and Shang et al. (2007); however such a blueshift does not seem so evident during our campaign. The light curves in Seasons 1 and 3 (and the entire light curve) show clear variations and can give reliable lag measurements. However, the lag measured from the entire light curve has the smallest uncertainties and is preferred for the BH mass determination. This yields a BH mass of $9.80^{+0.44}_{-0.46} \times 10^7 M_\odot$. Similar to PG 0049+171, we use the line profiles in the mean spectra to determine the velocity bins in the velocity-resolved analysis because of the relatively poor quality of the rms spectra. Its velocity-resolved lags generally show the signature of inflow (see Seasons 1 and 3; the lags at blue velocities are longer than the red ones).

PG 1211+143: The X-ray and UV observations suggest that this object has ultrafast outflows (Pounds et al. 2003; Danehkar et al. 2017). It is therefore interesting to investigate the kinematics of its BLR through RM. As a narrow-line Seyfert 1 galaxy, this object was monitored from 1991 to 1998 by Kaspi et al. (2000) and showed a Hβ time lag of $93.2^{+19.7}_{-29.9}$ days (Kaspi et al. 2005). Because the variation of its light curve in the previous campaign (Kaspi et al. 2000) was slow and the cadence was also not very high, the past result has relatively

Table 8
Hβ Asymmetry vs. BLR Kinematics

Target	$R_{\rm Fe}$	Hβ Asymmetry	BLR Kinematics
PG 0007+106	0.48	Symmetric	Keplerian/Virialized + weak inflow
PG 0049+171	0.13	Red	Keplerian/Virialized + weak outflow
PG 0923+129	0.53	Red	Inflow
PG 0947+396	0.33	Red	Keplerian/Virialized + weak inflow/outflow
PG 1001+054	0.89	Blue	Outflow
PG 1048+342	0.28	Red	Inflow
PG 1100+772	0.05	Red	Outflow
PG 1202+281	0.19	Red	Inflow
PG 1211+143	0.51	Blue	Inflow
PG 1310-108	0.23	Red	Unresolved
PG 1351+640	0.20	Red	Keplerian/Virialized
PG 1351+695	0.47	Symmetric	Keplerian/Virialized + inflow
PG 1501+106	0.26	Red	Inflow
PG 1534+580	0.21	Red	Complicated
PG 1613+658	0.57	Red	Inflow

Note. $R_{\rm Fe}$ is the flux ratio of Fe II and Hβ emission lines measured from our campaign (from an individual exposure with a high S/N ratio).

large uncertainties. Given the higher cadence in our campaign (∼4 days), the time lag becomes better defined, and we find it to be significantly shorter ($53.0^{+5.1}_{-5.8}$ days). The BH mass of $\log(M_\bullet/M_\odot) = 7.87^{+0.19}_{-0.19}$ given in Peterson et al. (2004) is larger than the value reported here ($2.14^{+0.21}_{-0.24} \times 10^7 M_\odot$ or $2.25^{+0.25}_{-0.28} \times 10^7 M_\odot$ from the FWHM or $\sigma_{\rm line}$ of the rms spectrum). The longer lags at blue velocities and the shorter at red (see Figure 18) suggest an inflowing BLR. This is the first determination of the BLR kinematics in this object.

PG1310−108: The Hβ time lag is reported here for the first time. This object historically showed an Hβ profile with a strong and extended red wing (Boroson & Green 1992). The Hβ light curve shows clear response to the varying continuum with a time lag of $12.8^{+1.7}_{-1.7}$ days. The BH mass measured from our campaign is $1.33^{+0.20}_{-0.22} \times 10^7 M_\odot$. Its lags at different velocities are not successfully resolved.

PG 1351+640: Kaspi et al. (2000) monitored this object in 1991–1998 but did not find a reliable Hβ lag measurement because of the relatively low cadence and large scatter of points in the light curve. Our data demonstrate significant variations and clear responses. The ICCF and MICA results are consistent with each other. The rms spectrum shows some residual signal around the [O III] wavelengths, which may originate from the variations in the contribution of the broad He Iλ4922,5016 lines (e.g., Jackson & Browne 1989) or a broad component of [O III] (e.g., Zakamska et al. 2016). The Fe II lines in this object are weak (see Table 8), so this residual signal is less likely from Fe IIλ4924,5018 lines. Because of the long-term variation timescale, we did not separate the light curves into different seasons. The time lag measured from the entire light curves in our campaign is $74.8^{+2.3}_{-2.3}$ days, and the BH mass is $1.52^{+0.07}_{-0.06} \times 10^8 M_\odot$. Similar to PG 0049+171, we used the line profile in the mean spectrum to determine the bins of velocity-resolved analysis because of the relatively lower S/N ratio of the rms spectrum. The inferred BLR kinematics is Keplerian/virialized motion.

PG 1351+695 (Mrk 279): Its Hβ variation amplitude in the present campaign is around $F_{\rm var} = 27\%$, which is stronger than the continuum variability ($F_{\rm var} = 12\%$), probably because the continuum flux is diluted by the contribution from its host galaxy. This object was first monitored from 1987 December to 1988 July with 39 points by Maoz et al. (1990), who reported a Hβ time lag of 12 ± 3 days. After that, it was monitored again from 1996 January to 1996 July by Santos-Lleó et al. (2001), giving a lag of $16.7^{+5.3}_{-5.6}$ days. More recently, Barth et al. (2015) reported a new RM measurement for this object from 2011 March to 2011 June, with a time lag consistent with the previous measurements (see also Williams et al. 2018). The time lag in the present paper is $19.9^{+1.0}_{-1.0}$ days, and the derived BH mass is $4.35^{+0.24}_{-0.23} \times 10^7 M_\odot$. Its velocity-resolved lags show a Keplerian disk or virialized motion of the BLR with probable contributions from inflow (see Figure 18).

PG 1501+106 (Mrk 841): We monitored this object for 4 yr (from 2017 to 2020). The light curve of the first season was published in Paper II. In the present paper, we slightly adjusted the window for measuring the Hβ fluxes in order to make sure that the variation signals in the rms spectra of all four seasons are covered. We used PyCALI (Li et al. 2014) to perform the intercalibration of the spectroscopic and photometric continuum light curves, which is different from the simple linear regression method in Paper II. This also makes the time lag measured from Season 1 slightly different but within 1σ uncertainties with respect to the value provided in Paper II. The variation of Season 2 is too weak to give a good constraint to the time lag; however Seasons 3 and 4 show clear and strong Hβ responses. It should be noted that the peak around JD ∼2458700 days in the Hβ light curve in Season 3 and the trough around JD ∼2459000 days in Season 4 are both narrower than their corresponding features in the continuum light curve (see Figure 14). This phenomenon makes the transfer function calculated through MICA for Seasons 3 and 4 have a second very broad component in addition to the primary narrow peak (see Figure 14). Although Season 3 has a very broad component in the transfer function from MICA, we still prefer to use the lag from this season in the BH mass measurement because its variability is the strongest during the campaign. The three methods (ICCF, χ^2, and MICA) yield generally consistent time lags for Season 3. The preferred BH mass measurement is $7.17^{+1.66}_{-0.79} \times 10^7 M_\odot$, which is slightly larger than the measurement in Paper II. U et al. (2022) monitored this object one year before our campaign although their light curves are of shorter duration. They obtained a BH mass measurement ($4.7^{+2.6}_{-1.6} \times 10^7 M_\odot$) slightly smaller than

ours in the present paper (but within 1σuncertainties). The velocity-resolved lags in Season 1 are not clear, as reported in Paper II, but both of the velocity-resolved lags in Seasons 3 and 4 show definite inflow signatures. This is consistent with the BLR kinematics reported by U et al. (2022).

PG 1534+580 (Mrk 290): This object was monitored before by Denney et al. (2010) who reported a time lag of 8.72 days in the rest frame. We measured a time lag of $25.4^{+2.0}_{-1.4}$ days, which is much longer than the result reported in Denney et al. (2010). It is not unexpected because, with a similar spectroscopic aperture, the fluxes in our campaign ($\sim 3.9 \times 10^{-15}$ erg s^{-1} cm^{-2} Å^{-1}) are much higher than those ($\sim 0.9 \times 10^{-15}$ erg s^{-1} cm^{-2} Å^{-1}) in Denney et al. (2010). The BH mass obtained from our campaign is $2.89^{+0.25}_{-0.19} \times 10^7 M_\odot$ and is almost the same as that determined by Denney et al. (2010). Denney et al. (2010) did not resolve the lags at different velocities. In our campaign, the data also do not allow us to give high-quality velocity-resolved lag measurements. However, the general structure of velocity-resolved lags implies complicated BLR geometry or kinematics.

PG 1613+658 (Mrk 876): This object was monitored during 1991–1998 (Kaspi et al. 2000) and a Hβ time lag of $40.1^{+15.0}_{-15.2}$ was reported (Kaspi et al. 2005). The trough of the Hβ light curve is in the gap in Season 1, which gives a poorer constraint to the time lag than from Season 2. The Hβ time lag measured from Season 2 (with better data quality) is $48.3^{+5.0}_{-3.8}$ days, which is similar to the value in (Kaspi et al. 2005) but much better constrained. The profile of broad Hβ shows a strong red asymmetry and does not show significant changes compared to that of Boroson & Green (1992), Erkens et al. (1995), and Kaspi et al. (2000). However, the Hβ profile plotted by De Robertis (1985) shows a much stronger red wing and a slightly blueshifted peak. The radius of the innermost part of its dusty torus ($334.1^{+42.4}_{-37.0}$ days) was measured by infrared reverberation mapping (Minezaki et al. 2019) and is larger by a factor of $\sim$7 compared with the BLR size in the present paper. Similar to the average lag determination, the gap in Season 1 makes the velocity-resolved lag measurement somewhat unreliable. The velocity-resolved lags of Season 2 indicate that its BLR is dominated by inflow.

4.2. H β Asymmetry and BLR Kinematics

To investigate if there is any correlation between the Hβ asymmetry and BLR kinematics, we make a short summary in Table 8. Although the size of the present sample is limited, it is obvious that the kinematics of the Keplerian/virialized motion and inflow is more common than outflow, in particular in the objects with broader Hβ (e.g., FWHM (Hβ) $\gtrsim$ 4000 km s^{-1}, corresponding to Population B in Marziani et al. 2003b), similar to the cases reported in the literature (e.g., Bentz et al. 2009; Denney et al. 2010; Grier et al. 2013; Du et al. 2016a). It appears that the asymmetry of the emission line does not directly correlate with the BLR kinematics (e.g., red-asymmetric lines can be associated with inflow, outflow, or Keplerian/virialized BLR kinematics). This is consistent with the fact that the emission-line profile is the integration of the clouds in BLR and has relatively stronger degeneracy than the velocity-resolved lags for the BLR geometry and kinematics. The flux ratios of Fe II (from 4434 to 4684 Å) and Hβ lines ($R_{\rm Fe}$) are also listed in Table 8.

Parameter A listed in Table 1 is measured from an individual exposure with a high S/N ratio. We have checked that the variation in A is relatively weak (although not zero) for each object during the campaign. The "blue" or "red" asymmetry did not change in our observations. It is the same as expected because the varying part of the emission line is only a small portion of the entire profile. This can be justified from the much weaker emission lines in the rms spectra with respect to those in the mean spectra (see Figures 2–16). Therefore, it is enough to list parameter A measured from one individual exposure for exhibiting the blue or red asymmetry of the emission-line profiles for the present sample.

5. Summary

In this third paper of the series, we present the RM measurements of 15 PG targets from the MAHA project. Our campaign has both long-term duration (spans from 1 to 5 yr for different objects) and high cadence. We successfully measure reverberation time lags between the continuum and Hβ light curves for individual seasons using three different methods (ICCF, χ^2, and MICA). ICCF and MICA show more consistent results, while the χ^2 method demonstrates slightly larger scatter. The BH masses of PG 0049+171, PG 0923+129, PG 0947+396, PG 1001+054, PG 1048+342, PG 1100+772, PG 1202+281, PG 1310−108, PG 1351+640 are reported for the first time. The velocity-resolved lags of the objects are also measured and show very diverse kinematics (virialized, inflow, and outflow signatures). The results from the present sample suggest that the BLR kinematics of Keplerian/virialized motion and inflow is more common than that of outflow. Future BLR modeling will investigate their BLR geometry and kinematics in more detail.

We thank the anonymous referee for valuable comments that improved the article. We thank WIRO engineers James Weger, Conrad Vogel, and Andrew Hudson for their indispensable and invaluable assistance. We also acknowledge the valuable support from the staff of the Lijiang 2.4 m telescope, CAHA 2.2 m telescope, Asiago 1.82 m telescope, and SAAO 1.9 m telescope. Funding for the Lijiang 2.4 m telescope has been provided by CAS and the Peoples Government of Yunnan Province. This work is partly based on observations collected at the Centro Astronómico Hispanoen Andalucía (CAHA) at Calar Alto, operated jointly by the Andalusian Universities and the Instituto de Astrofísica de Andalucía (CSIC). This research is based in part on observations collected at Copernico telescope (Asiago, Italy) of the INAF—Osservatorio Astronomico di Padova. We thank the South African Astronomical Observatory for the allocation of telescope time, and Francois van Wyk for obtaining some of the spectra. We acknowledge the support by the National Science Foundation of China through grants NSFC-12022301, -11991051, -11991054, -11873048, -11833008, by National Key R&D Program of China (grants 2016YFA0400701), by grant No. QYZDJ-SSW-SLH007 from the Key Research Program of Frontier Sciences, Chinese Academy of Sciences (CAS), by the Strategic Priority Research Program of CAS grant No.XDB23010400, and by the International Partnership Program of CAS, grant No.113111 KYSB20200014. L.C.H. was supported by the National Science Foundation of China (11721303, 11991052) and the National Key R&D Program of China (2016YFA0400702). M.B. enjoyed support from the Chinese Academy of Sciences Presidents International Fellowship Initiative, grant No. 2018VMA0005. YRL acknowledges financial support from the National Natural Science Foundation of China through

grant NSFC-11922304 and from the Youth Innovation Promotion Association CAS. H.C. acknowledges financial support from grant NSFC-12122305. We also acknowledge support from a University of Wyoming Science Initiative Faculty Innovation Seed grant. This work is supported by the National Science Foundation under REU grant AST 1852289. T.E.Z. acknowledges support from NSF grant 1005444I.

This work is also based on observations obtained with the Samuel Oschin 48 inch Telescope at the Palomar Observatory as part of the Zwicky Transient Facility project. ZTF is supported by the National Science Foundation under grant No. AST-1440341 and a collaboration including Caltech, IPAC, the Weizmann Institute for Science, the Oskar Klein Center at Stockholm University, the University of Maryland, the University of Washington, Deutsches Elektronen-Synchrotron and Humboldt University, Los Alamos National Laboratories, the TANGO Consortium of Taiwan, the University of Wisconsin at Milwaukee, and Lawrence Berkeley National Laboratories. Operations are conducted by COO, IPAC, and UW. This work makes use of the public data from ASAS-SN project. ASAS-SN is supported by the Gordon and Betty Moore Foundation through grant GBMF5490 to the Ohio State University, and NSF grants AST-1515927 and AST-1908570. Development of ASAS-SN has been supported by NSF grant AST-0908816, the Mt. Cuba Astronomical Foundation, the Center for Cosmology and AstroParticle Physics at the Ohio State University, the Chinese Academy of Sciences South America Center for Astronomy (CAS- SACA), the Villum Foundation, and George Skestos.

Software: DASpec (https://github.com/PuDu-Astro/DASpec), PyCALI (Li et al. 2014), MICA (Li et al. 2016).

ORCID iDs

Dong-Wei Bao https://orcid.org/0000-0003-2024-1648
Michael S. Brotherton https://orcid.org/0000-0002-1207-0909
Pu Du https://orcid.org/0000-0002-5830-3544
Jacob N. McLane https://orcid.org/0000-0003-1081-2929
Bi-Xuan Zhao https://orcid.org/0000-0002-1007-1991
Sha-Sha Li https://orcid.org/0000-0003-3823-3419
Yu-Yang Songsheng https://orcid.org/0000-0003-4042-7191
Yan-Rong Li https://orcid.org/0000-0001-5841-9179
Bo-Wei Jiang https://orcid.org/0000-0003-3825-0710
David H. Kasper https://orcid.org/0000-0003-0534-6388
William T. Chick https://orcid.org/0000-0002-8818-6780
Jaya Maithil https://orcid.org/0000-0002-4423-4584
H. A. Kobulnicky https://orcid.org/0000-0002-4475-4176
D. A. Dale https://orcid.org/0000-0002-5782-9093
Hartmut Winkler https://orcid.org/0000-0003-2662-0526
Paola Marziani https://orcid.org/0000-0002-6058-4912
Mauro D'Onofrio https://orcid.org/0000-0001-6441-9044
Ming Xiao https://orcid.org/0000-0001-5981-6440
Bożena Czerny https://orcid.org/0000-0001-5848-4333
Jesús Aceituno https://orcid.org/0000-0003-0487-1105
Luis C. Ho https://orcid.org/0000-0001-6947-5846
Jian-Min Wang https://orcid.org/0000-0001-9449-9268

References

Barth, A. J., Bennert, V. N., Canalizo, G., et al. 2015, ApJS, 217, 26
Barth, A. J., Pancoast, A., Bennert, V. N., et al. 2013, ApJ, 769, 128
Begelman, M. C., Blandford, R. D., & Rees, M. J. 1980, Natur, 287, 307
Bentz, M. C., Denney, K. D., Grier, C. J., et al. 2013, ApJ, 767, 149
Bentz, M. C., Walsh, J. L., Barth, A. J., et al. 2008, ApJ, 689, L21
Bentz, M. C., Walsh, J. L., Barth, A. J., et al. 2009, ApJ, 705, 199
Blandford, R. D., & McKee, C. F. 1982, ApJ, 255, 419
Bon, E., Jovanović, P., Marziani, P., et al. 2012, ApJ, 759, 118
Boroson, T. A., & Green, R. F. 1992, ApJS, 80, 109
Boroson, T. A., Persson, S. E., & Oke, J. B. 1985, ApJ, 293, 120
Brewer, B. J., Partay, L. B., & Csanyi, G. 2011, Stat. Comput., 21, 649
Brotherton, M. S., Du, P., Xiao, M., et al. 2020, ApJ, 905, 77
Bruzual, G., & Charlot, S. 2003, MNRAS, 344, 1000
Capriotti, E., Foltz, C., & Byard, P. 1979, ApJ, 230, 681
Chen, K., & Halpern, J. P. 1989, ApJ, 344, 115
Chen, K., Halpern, J. P., & Filippenko, A. V. 1989, ApJ, 339, 742
Clavel, J., Reichert, G. A., Alloin, D., et al. 1991, ApJ, 366, 64
Czerny, B., Hryniewicz, K., Maity, I., et al. 2013, A&A, 556, A97
Czerny, B., Olejak, A., Rałowski, M., et al. 2019, ApJ, 880, 46
Dalla Bontà, E., Peterson, B. M., Bentz, M. C., et al. 2020, ApJ, 903, 112
Danehkar, A., Nowak, M. A., Lee, J. C., et al. 2017, ApJ, 853, 165
De Robertis, M. 1985, ApJ, 289, 67
De Rosa, G., Fausnaugh, M. M., Grier, C. J., et al. 2018, ApJ, 866, 133
Denney, K. D., Peterson, B. M., Pogge, R. W., et al. 2009, ApJL, 704, L80
Denney, K. D., Peterson, B. M., Pogge, R. W., et al. 2010, ApJ, 721, 715
Du, P., Brotherton, M. S., Wang, K., et al. 2018a, ApJ, 869, 142
Du, P., Hu, C., Lu, K.-X., et al. 2014, ApJ, 782, 45
Du, P., Hu, C., Lu, K.-X., et al. 2015, ApJ, 806, 22
Du, P., Lu, K.-X., Hu, C., et al. 2016a, ApJ, 820, 27
Du, P., Lu, K.-X., Zhang, Z.-X., et al. 2016b, ApJ, 825, 126
Du, P., & Wang, J.-M. 2019, ApJ, 886, 42
Du, P., Zhang, Z.-X., Wang, K., et al. 2018b, ApJ, 856, 6
Edelson, R., Turner, T. J., Pounds, K., et al. 2002, ApJ, 568, 610
Eracleous, M., Boroson, T. A., Halpern, J. P., & Liu, J. 2012, ApJS, 201, 23
Eracleous, M., Livio, M., Halpern, J. P., & Storchi-Bergmann, T. 1995, ApJ, 438, 610
Erkens, U., Wagner, S. J., Alloin, D., et al. 1995, A&A, 296, 90
Fausnaugh, M. M. 2017, PASP, 129, 024007
Fausnaugh, M. M., Grier, C. J., Bentz, M. C., et al. 2017, ApJ, 840, 97
Ferland, G. J., Netzer, H., & Shields, G. A. 1979, ApJ, 232, 382
Fu, H., & Stockton, A. 2009, ApJ, 690, 953
Gaskell, C. M., & Peterson, B. M. 1987, ApJS, 65, 1
Gaskell, C. M., & Sparke, L. S. 1986, ApJ, 305, 175
Gilbert, G. M., Riley, J. M., Hardcastle, M. J., et al. 2004, MNRAS, 351, 845
Grier, C. J., Pancoast, A., Barth, A. J., et al. 2017, ApJ, 849, 146
Grier, C. J., Peterson, B. M., Horne, K., et al. 2013, ApJ, 764, 47
Grier, C. J., Peterson, B. M., Pogge, R. W., et al. 2012, ApJ, 755, 60
Grier, C. J., Trump, J. R., Shen, Y., et al. 2017, ApJ, 851, 21
Ho, L. C., & Kim, M. 2014, ApJ, 789, 17
Horne, K., De Rosa, G., Peterson, B. M., et al. 2021, ApJ, 907, 76
Hu, C., Du, P., Lu, K. X., et al. 2015, ApJ, 804, 128
Hu, C., Li, S.-S., Guo, W.-J., et al. 2020a, ApJ, 905, 75
Hu, C., Li, Y. R., Du, P., et al. 2020b, ApJ, 890, 71
Hu, C., Wang, J.-M., Ho, L. C., et al. 2008, ApJ, 687, 78
Jackson, N., & Browne, I. W. A. 1989, MNRAS, 236, 97
Ji, X., Lu, Y., Ge, J., Yan, C., & Song, Z. 2021, ApJ, 910, 101
Kaspi, S., Brandt, W. N., Maoz, D., et al. 2017, FrASS, 4, 31
Kaspi, S., Brandt, W. N., Maoz, D., et al. 2021, ApJ, 915, 129
Kaspi, S., Maoz, D., Netzer, H., et al. 2005, ApJ, 629, 61
Kaspi, S., Smith, P. S., Netzer, H., et al. 2000, ApJ, 533, 631
Kochanek, C. S., Shappee, B. J., Stanek, K. Z., et al. 2017, PASP, 129, 104502
Kovačević, A. B., Wang, J.-M., & Popović, L. Č. 2020, A&A, 635, A1
Li, H. Z., Xie, G. Z., Dai, H., et al. 2010, NewA, 15, 254
Li, S.-S., Yang, S., Yang, Z.-X., et al. 2021, ApJ, 920, 9
Li, Y.-R., Songsheng, Y.-Y., Qiu, J., et al. 2018, ApJ, 869, 137
Li, Y.-R., Wang, J.-M., & Bai, J.-M. 2016, ApJ, 831, 206
Li, Y.-R., Wang, J.-M., Ho, L. C., et al. 2016, ApJ, 822, 4
Li, Y.-R., Wang, J.-M., Ho, L. C., Du, P., & Bai, J.-M. 2013, ApJ, 779, 110
Li, Y. R., Wang, J. M., Hu, C., Du, P., & Bai, J. M. 2014, ApJL, 786, L6
Lira, P., Kaspi, S., Netzer, H., et al. 2018, ApJ, 865, 56
Lu, K.-X., Du, P., Hu, C., et al. 2016, ApJ, 827, 118
Maoz, D., Netzer, H., Leibowitz, E., et al. 1990, ApJ, 351, 75
Marziani, P., Sulentic, J. W., Zamanov, R., et al. 2003a, ApJS, 145, 199
Marziani, P., Zamanov, R. K., Sulentic, J. W., & Calvani, M. 2003b, MNRAS, 345, 1133
Masci, F. J., Laher, R. R., Rusholme, B., et al. 2019, PASP, 131, 018003
Minezaki, T., Yoshii, Y., Kobayashi, Y., et al. 2019, ApJ, 886, 150
Netzer, H., & Trakhtenbrot, B. 2007, ApJ, 654, 754

Oknyansky, V. L., Brotherton, M. S., Tsygankov, S. S., et al. 2021, MNRAS, 505, 1029
Onken, C. A., Ferrarese, L., Merritt, D., et al. 2004, ApJ, 615, 645
Pancoast, A., Brewer, B. J., & Treu, T. 2011, ApJ, 730, 139
Pancoast, A., Brewer, B. J., Treu, T., et al. 2014, MNRAS, 445, 3073
Peterson, B., Wanders, I., Horne, K., et al. 1998, PASP, 110, 660
Peterson, B. M. 1993, PASP, 105, 247
Peterson, B. M., Berlind, P., Bertram, R., et al. 2002, ApJ, 581, 197
Peterson, B. M., Ferrarese, L., Gilbert, K. M., et al. 2004, ApJ, 613, 682
Planck Collaboration, Ade, P. A. R., Aghanim, N., et al. 2014, A&A, 571, A16
Planck Collaboration, Aghanim, N., Akrami, N., et al. 2020, A&A, 641, A6
Pounds, K. A., Reeves, J. N., King, A. R., et al. 2003, MNRAS, 345, 705
Press, W. H., Teukolsky, S. A., Vetterling, W. T., & Flannery, B. P. 1992, Numerical Recipes in FORTRAN. The Art of Scientific Computing
Rafter, S. E., Kaspi, S., Behar, E., Kollatschny, W., & Zetzl, M. 2011, ApJ, 741, 66
Rakshit, S., Woo, J. H., Gallo, E., et al. 2019, ApJ, 886, 93
Rodríguez-Pascual, P. M., Alloin, D., Clavel, J., et al. 1997, ApJS, 110, 9
Romero, G. E., Chajet, L., Abraham, Z., & Fan, J. H. 2000, A&A, 360, 57
Santos-Lleó, M., Clavel, J., Schulz, B., et al. 2001, A&A, 369, 57
Schlafly, E. F., & Finkbeiner, D. P. 2011, ApJ, 737, 103
Schmidt, M., & Green, R. F. 1983, ApJ, 269, 352
Shang, Z., Wills, B. J., Wills, D., & Brotherton, M. S. 2007, AJ, 134, 294
Shappee, B. J., Prieto, J. L., Grupe, D., et al. 2014, ApJ, 788, 48
Shen, Y., Horne, K., Grier, C. J., et al. 2016, ApJ, 818, 30
Shen, Y., & Loeb, A. 2010, ApJ, 725, 249
Songsheng, Y.-Y., Xiao, M., Wang, J.-M., & Ho, L. C. 2020, ApJS, 247, 3
Stockton, A., & Mackenty, J. W. 1983, Natur, 305, 678
Storchi-Bergmann, T., Nemmen da Silva, R., Eracleous, M., et al. 2003, ApJ, 598, 956
Sulentic, J. W. 1989, ApJ, 343, 54
Teräsranta, H., Wiren, S., Koivisto, P., Saarinen, V., & Hovatta, T. 2005, A&A, 440, 409
U, V., Barth, A. J., Vogler, H. A., et al. 2022, ApJ, 925, 52
van Groningen, E., & Wanders, I. 1992, PASP, 104, 700
Wang, J.-M., Du, P., Brotherton, M. S., et al. 2017, NatAs, 1, 775
Wang, J.-M., Songsheng, Y.-Y., Li, Y.-R., & Yu, Z. 2018, ApJ, 862, 171
Williams, P. R., Pancoast, A., Treu, T., et al. 2018, ApJ, 866, 75
Winkler, H., & Paul, B. 2017, arXiv:1708.02056
Woo, J.-H., Cho, H., Gallo, E., et al. 2019, NatAs, 3, 755
Woo, J.-H., Treu, T., Barth, A. J., et al. 2010, ApJ, 716, 269
Woo, J.-H., Yoon, Y., Park, S., Park, D., & Kim, S. C. 2015, ApJ, 801, 38
Xiao, M., Du, P., Horne, K., et al. 2018, ApJ, 864, 109
Yu, Z., Martini, P., Penton, A., et al. 2021, MNRAS, 507, 3771
Zajaček, M., Czerny, B., Martinez-Aldama, M. L., et al. 2020, ApJ, 896, 146
Zajaček, M., Czerny, B., Martinez-Aldama, M. L., et al. 2021, ApJ, 912, 10
Zakamska, N. L., Hamann, F., Pâris, I., et al. 2016, MNRAS, 459, 3144
Zhang, Z. X., Du, P., Smith, P. S., et al. 2018, ApJ, 876, 49